Simultaneous Optimal Bottom Linewidth and Side-Wall Curvature Control of Wet Etching

Bo Zhou and W. Fred Ramirez
Dept. of Chemical Engineering, University of Colorado at Boulder, Boulder, CO 80309

Etching is one of the critical steps in the fabrication of microelectronics devices. A time-optimal control problem with a dual-term terminal cost including both bottom linewidth and side-wall curvature is formulated to implement an optimal open-width design principle. A singular-arc solution does not exist and the control action is bang-bang. The optimal switching time is analytically calculated. The feasibility and effectiveness of this technique are illustrated by simulation studies. This design and control philosophy can easily be applied to other microelectronics manufacturing processes.

Introduction

Etching is one of the critical steps in the manufacturing of microelectronics devices, since images are irreversibly transferred into a permanent film on the substrate (Moreau, 1988). Currently, most etching processes are operated on a trial-and-error basis, and automatic control of the process is not common. Important process variables directly related to the product quality and process productivity, such as, the bottom linewidth, the side-wall curvature, and the cycle time, are not normally directly controlled.

An early application of advanced process control in lithography is that of Boehm (1982). Four nonlinear process variables of a dry-etch process were adaptively controlled with a recursive least-squares estimation method combined with a deadbeat controller. Although neither the bottom linewidth nor the side-wall curvature were among those four controlled variables, the impact of this research is significant.

Direct bottom linewidth control in lithography was made by Lauchlan et al. (1985) for photoresist development. Optical interferometry was used to measure the film thickness in real time. By identifying the time to surface breakthrough, also called the *control point time* (CPT), and relating this value to the required total development time needed to achieve the desired bottom linewidth, process control is achieved. A calibration run is performed for each masking level to determine the functional relationship between CPT and the total development time. The total development time completely relies on real-time measurements and trial-and-error experiments.

On-line adaptive control of bottom linewidth in lithography was studied by Carroll and Ramirez (1990, 1993). They used state and parameter identification and adaptive control to achieve optimal process control of positive photoresist development. Mathematical models were used in conjunction with on-line development penetration data based on optical interferometry. A model describing the postbreakthrough dissolution was used to determine the total development time, based on the knowledge of the development rate parameter. Experimental results were reported that the control policy and identification algorithm provided tight adaptive control on the desired bottom linewidth, despite continually changing environmental conditions. The control of side-wall curvature was not addressed in their work.

An adaptive run-to-run control strategy of photolithography was reported by Crisalle et al. (1992). A lumped-parameter model was used to describe the relationship between the critical dimension (the controlled variable) and the exposure energy (the manipulated variable). Model parameters were updated using least-square estimation based on direct measurement of the critical dimension by scanning electron microscopy (SEM). The adaptive controller was a nonlinear model-inversion controller. The performance of this control scheme was studied by simulation.

In this article, an optimal design principle that is capable of simultaneous bottom linewidth and side-wall curvature control (Zhou and Ramirez, 1996a) is described. An optimal control problem is then formulated and solved. The performance index of this problem represents the three major quality and economic concerns in the manufacturing process, namely:

- Minimize the deviation from a setpoint for bottom linewidth.

Correspondence concerning this article should be addressed to W. F. Ramirez.

• Minimize the deviation from a setpoint for side-wall curvature.

• Minimize the cycle time.

The first two are the key quality parameters, while the cycle time is the major factor that affects the process throughput, and therefore affects the productivity and profitability of the process. The control action is bang-bang, and a singular-arc solution is shown not to exist. The optimal switching time from etching to rinsing, in the sense that an optimal trade-off among the three criteria considered is reached, can be calculated analytically.

Optimal Open-Width Design Principle

Common practice in wet etching and lithography is to have the open width in the mask the same as the desired bottom linewidth after resist development. Although the open width in the mask is sometimes changed to cope with the diffraction effect during the photoresist exposure process, the opening in the resist after development is still designed to be of the desired bottom linewidth in the film to be etched. Both strategies can be called the exact open width (EOW) problem.

Based on an isotropic etch assumption (Kern and Deckert, 1978; Lichtenberg et al., 1993), the etch profile can be simulated by Fermat's principle of least time (Morgan, 1953; Oh et al., 1981), or Barouch's least-action principle (Barouch and Bradie, 1988), both of which lead to the conclusion that the contour of the side wall is a quarter of a circle centered at the edge of photoresist layer (Carrier and Pearson, 1976; Carroll, 1990).

Only the bottom linewdith is addressed in the EOW problem. The side-wall curvature, η, defined here as

$$\eta = \frac{d}{R}, \tag{1}$$

is unity when the desired linewidth is reached using EOW. Here d is the actual film thickness, and R is the undercut. In most cases, a smaller curvature is more desireable. It facilitates the succeeding liftoff operations, helps increase device density by decreasing undesired undercut, and more importantly, improves performance of numerous devices. As can be seen in Figure 1, the side-wall curvature decreases as the undercut increases after breakthrough. Zhou and Ramirez (1996a) suggested that by controlling the overetch time, the side-wall curvature can be controlled, and that following optimal open width (OOW) design principle was proposed:

Given the design film thickness, d_s, desired bottom linewidth, L_s, and desired side-wall curvature, η_s, the optimal open width in the masking layer, L_m, can be calculated by:

$$L_m = L_s - 2\sqrt{\left(\frac{d_s}{\eta_s}\right)^2 - d_s^2}\,. \tag{2}$$

Thus, by selecting the open width in the masking layer, both linewidth and curvature can reach ideal values. The total etch time, t_f, can be solved numerically from

$$\frac{d_s}{\eta_s} = d_s + \int_{t_0}^{t_f} r\,dt, \tag{3}$$

where t_0 is the breakthrough time, and r is the etch rate. The breakthrough time, t_0, is detected using optical interferometry (Lauchlan et al., 1985; Carroll, 1990).

An example is provided in Figure 2, where the ratio of the desired bottom linewidth, L_s, to the film thickness, d_s, is 10, and the setpoint for the side-wall curvature, η_s, is 0.5. According to Eq. 2, the actual opening in the masking layer is

$$L_m = 6.536\ d_s. \tag{4}$$

The side-wall contour thus obtained is illustrated in Figure 2 by arc 1. Arc 2 represents the side-wall profile if the EOW is used.

A desirable byproduct of the OOW design principle is that with a smaller opening in the masking layer, a larger contact area is provided between the masking layer and the film to be etched, thus helping solve, or at least alleviate, the lifting problem, which is a common concern in etching processes. For example, in Figure 2, the contact area before etch starts is OOW1, if the OOW design principle is used, and EOW1 for EOW. The contact area for the OOW case is OOW2 when the desired bottom linewidth is reached, and EOW2 for the EOW case. Actually, during the whole process, OOW always provides larger contact area than EOW between the photoresist and the alumina layer.

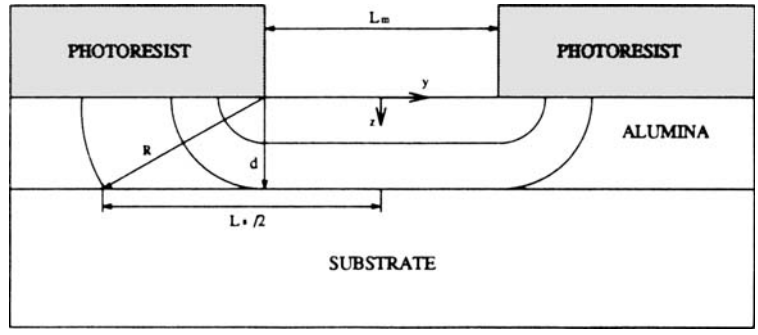

Figure 1. Side-wall profiles during isotropic etch.

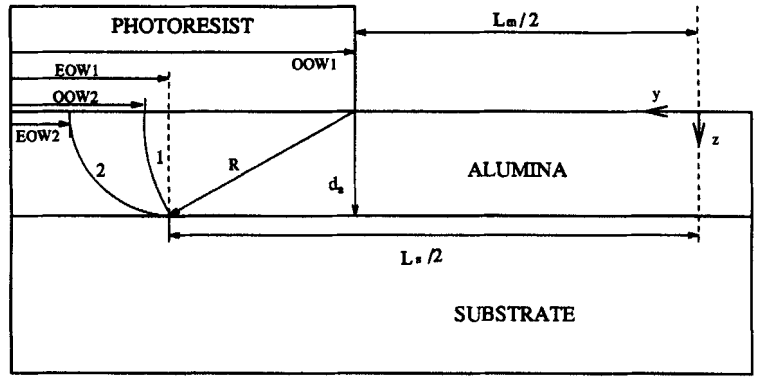

Figure 2. Example of OOW design.

The Optimal Control Problem

The following optimal control problem is formulated to represent the three objectives discussed in the first section:

$$\min J = w_1(L(t_f) - L_s)^2 + w_2(\eta(t_f) - \eta_s)^2 + \int_{t_0}^{t_f} dt, \quad (5)$$

with the equality constraint of the process model:

$$\dot{R}(t) = r, \quad (6)$$

where

$$0 \le r \le r_{\max}. \quad (7)$$

Here, L_s and η_s are setpoints for the bottom linewidth and the side-wall curvature, respectively, and

$$L(t) = L_m + 2\sqrt{R(t)^2 - d^2} \quad (8)$$

$$\eta(t) = \frac{d}{R(t)} \quad (9)$$

$$R(t) = d + \int_{t_0}^{t} r\, dt. \quad (10)$$

The etch rate, r, is the control variable, which is a function of etchant temperature and concentration, and $r_{\max}$ the maximum etching rate under the specified etching condition. The equality constraint, Eq. 6, is an experimentally derived model (Zhou and Ramirez, 1996b) that describes the reaction kinetics of the etching process. The parameters w_1 and w_2 are weighting coefficients that reflect the relative importance of the various terms in the performance functional.

Notice that the actual film thickness, d, is used in Eqs. 8 to 10. In a manufacturing environment, wafers may reach the etching step with film thickness different than the design value, d_s. The open width in the masking layer, L_m, is always calculated from Eq. 2 using the design film thickness, d_s.

To make the weighting coefficients more meaningful and comparable, the problem is rewritten in dimensionless form:

$$\min J^* = w_1^*(L^*(t_f^*) - 1)^2 + w_2^*(\eta^*(t_f^*) - 1)^2 + \int_1^{t_f^*} dt^*, \quad (11)$$

with the state equation

$$\dot{R}^*(t^*) = \beta r^* \quad (12)$$

and

$$0 \le r^* \le 1, \quad (13)$$

where

$$L^* = \frac{L}{L_s} \quad (14)$$

$$\eta^* = \frac{\eta}{\eta_s} \quad (15)$$

$$t^* = \frac{t}{t_0} \quad (16)$$

$$t_f^* = \frac{t_f}{t_0} \quad (17)$$

$$r^* = \frac{r}{r_{\max}} \quad (18)$$

$$R^* = \frac{R}{R_s} \quad (19)$$

$$R_s = \frac{d_s}{\eta_s} \quad (20)$$

$$\beta = \frac{r_{\max}}{R_s}. \quad (21)$$

Here, β is a dimensional coefficient.

The Hamiltonian (Ramirez, 1994) has the form:

$$H = \lambda \beta r^* + 1, \quad (22)$$

where λ is the costate variable. Since the Hamiltonian is linear in the control variable, r^*, either the control action is bang-bang or there exists a singular arc.

The costate variable is defined by

$$\dot{\lambda} = -\frac{\alpha H}{\partial R^*} = 0, \tag{23}$$

which indicates that λ is a constant and does not change sign.

The transversality condition gives

$$\left[\frac{\partial h}{\partial R^*}(t_f^*) - \lambda(t_f^*)\right]\delta R^*(t_f^*) + \left[H(t_f^*) + \frac{\partial h}{\partial t^*}(t_f^*)\right]\delta t_f^* = 0, \tag{24}$$

where

$$h = w_1^*(L^*(t_f^*)-1)^2 + w_2^*(\eta^*(t_f^*)-1)^2. \tag{25}$$

Since $\delta R^*(t_f^*)$ and δt_f^* are unknown and free, we have

$$\frac{\partial h}{\partial R^*}(t_f^*) - \lambda(t_f^*) = 0 \tag{26}$$

$$H(t_f^*) + \frac{\partial h}{\partial t^*}(t_f^*) = 0. \tag{27}$$

Also, h is not explicit in t^* (Eq. 25), therefore

$$\frac{\partial h}{\partial t^*} = 0, \tag{28}$$

which leads to

$$H(t_f^*) = 0. \tag{29}$$

With constraints on the control, Pontryagin's Maximum Principle (Pontryagin et al., 1962) is then applied to find the optimal solution, which is bang-bang control given by

$$r^* = 1, \quad \text{if} \quad \lambda < 0 \tag{30}$$

$$r^* = 0, \quad \text{if} \quad \lambda > 0. \tag{31}$$

Since λ is a constant and retains the same sign, r^* equals either unity or zero, and does not switch between these two limits within the time domain $[1, t_f^*]$.

Combining Eqs. 22 and 29 yields

$$H(t_f^*) = \lambda(t_f^*)\beta r^*(t_f^*) + 1 = 0. \tag{32}$$

The minimum control action, $r^* = 0$, is impossible since it violates Eq. 32. It is also physically impossible over the entire time domain, since it is the condition of no etching. Therefore, the feasible bang-bang control is the maximum control

$$r^* = 1, \tag{33}$$

and the final costate becomes

$$\lambda(t_f^*) = -\frac{1}{\beta}. \tag{34}$$

Substituting $\lambda(t_f^*)$ into the transversality condition (Eq. 26), gives

$$\frac{\partial h}{\partial R^*}(t_f^*) = -\frac{1}{\beta}, \tag{35}$$

which is equivalent to

$$4w_1^*\left(\frac{L_m + 2R_s\sqrt{(R^*)^2 - (d/R_s)^2}}{L_s} - 1\right) \times \frac{R_s}{L_s}\frac{R^*}{\sqrt{(R^*)^2-(d/R_s)^2}} + 2w_2^*\left(\frac{d}{R^*R_s\eta_s} - 1\right)\frac{d_s}{\eta_s^2}\left(-\frac{d/R_s^2}{(R^*)^2}\right) = -\frac{1}{\beta}. \tag{36}$$

This nonlinear equation can be solved for $R^*(t_f^*)$ using a general root-finding algorithm. The shape of the nonlinear function of Eq. 36 is depicted in Figure 3 for typical values of $\eta_s = 0.5$, $L_s = 10$ μm, and $d = d_s = 1$ μm, with the ratio of w_1^*/w_2^* changing from 0.5 to 10. It can be seen that within the range of interest, this nonlinear function is monotone and has a single root. Simulations with other parameter values show a similar pattern. A reasonable initial guess for R_s^* is 1.

The dimensional value for $R(t_f)$ can be easily obtained by multiplying $R^*(t_f^*)$ by R_s, then using Eq. 10 to calculate the optimal stopping time t_f. Since $r = r_{\max}$ in the dimensional form, Eq. 10 becomes

$$R(t_f) = d + r_{\max}(t_f - t_0) \tag{37}$$

and

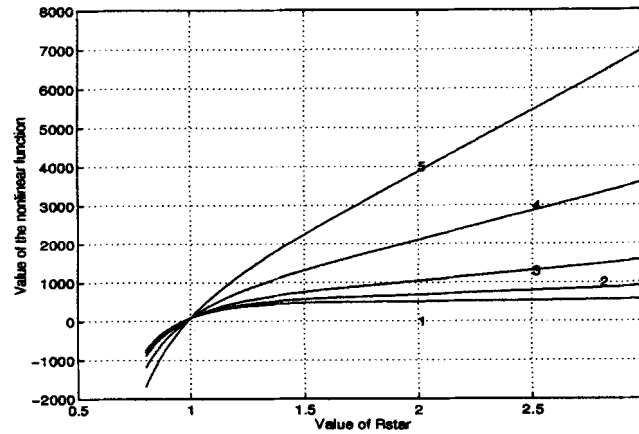

Figure 3. General shape of the nonlinear function resulting from the optimal control problem.

Line 1: $w_1^*/w_2^* = 0.5$; line 2: $w_1^*/w_2^* = 1.0$; line 3: $w_1^*/w_2^* = 2.0$; line 4: $w_1^*/w_2^* = 5.0$; line 5: $w_1^*/w_2^* = 10.0$.

$$t_f = t_0 + \frac{R(t_f) - d}{r_{\max}}. \tag{38}$$

The existance of a singular solution ($\lambda = 0$) is not possible since this solution contradicts the final Hamiltonian relationship of Eq. 32.

Simulation Studies

To illustrate the effectiveness of the proposed design and control technique, an example coming from the manufacturing of read head in the tape drive is simulated in this section. As shown in the previous discussion, in order to calculate the optimal stopping time, besides all the design parameters (L_s, η_s, and d_s), two more variables, $r_{\max}$ and d, need to be specified. Here, we assume that these variables are known. When the optimal control system is implemented, both variables can be estimated by an augmented Kalman filter using data from an end-point detector (Zhou and Ramirez, 1996a).

As is common in industrial operations, the total etch time by EOW is composed of two parts, an estimated breakthrough time using the actual film thickness, d, and the maximum etch rate, $r_{\max}$, plus a 15% overetch time to ensure breakthrough and a clean breakthrough surface. The main reason to use the 15% overetch time is that residual "islands," which could be fatal, may occur at the breakthrough time. Since the OOW design principle results in excessive overetching, no further overetching is needed.

Case I. This case simulates the scenario where the actual film thickness is of the design value and the cycle time is not important. Therefore,

$$d = d_s \tag{39}$$

$$w_1^*, w_2^* \gg 1. \tag{40}$$

Table 1 summarizes the simulation parameters. Table 2 shows the OOW simulation results along with the results of the EOW reference case. It is obvious that OOW is capable of controlling the bottom linewidth and side-wall curvature simultaneously. Both reach their setpoints. However, the cycle time is 1.7 times that of EOW.

Case II. If the cycle time is a factor to be considered, the weighting coefficients, w_1^* and w_2^*, can be adjusted to obtain the optimal trade-off among the linewidth, wall curvature, and cycle time. Table 3 lists the parameters used when the relative importance of the linewidth to curvature to time is 1,000:40:1. Table 4 shows the results calculated from the optimal control problem. A 12.5% reduction in the cycle time is obtained when compared to Case I, at the price that linewidth and wall curvature are 6.4% and 15.7% away from setpoints, respectively.

Case III. The optimal controller can also handle process drifts in film thickness, which is inevitable in a manufacturing environment. If the actual film thickness, d, is less than the design value, d_s, using the parameters listed in Table 5, we have the results in Table 6. While the total etch time of OOW is almost twice that of EOW, the linewidth of OOW is very close to its setpoint, with only 0.57% deviation. EOW results in a 10% deviation. Also the wall curvature of OOW is close to its setpoint with a deviation of 6.6%, which is much better than that of EOW. It is possible to retune w_1^* and w_2^* to reduce the cycle time if it deserves more weight.

Case IV. This simulation studies the case where d is greater than d_s. Again, sacrificing the cycle time brings the final linewidth and curvature into 0.03% and 6.6% of their setpoints, respectively. Again, OOW operation is much preferable to EOW operation in terms of meeting target performance specification. As more weight is assigned to the linewidth, it is closer to its desired value. This would reflect the general quality requirement in the fabrication of read heads in the tape drive. Parameters and results for Case IV are lists in Tables 7 and 8.

From all the cases studied, it can be deducted that the OOW operational policy allows for the simultaneous control of both linewidth and side-wall curvature. The EOW opera-

Table 1. Parameters for Case I*

L_s (μm)	η_s	d_s(μm)	d(μm)	$r_{\max}$(Å/min)	w_1^*	w_2^*
10	0.5	1	1	250	1,000,000	1,000,000

*$d = d_s$, $w_1^*, w_2^* \gg 1$.

Table 2. Results for Case I*

OOW			EOW		
$L(t_f)$ (μm)	$\eta(t_f)$	t_f (min)	$L(t_f)$ (μm)	$\eta(t_f)$	t_f (min)
10.00	0.50	79.99	11.14	0.87	46

*$d = d_s$, $w_1^*, w_2^* \gg 1$.

Table 3. Parameters for Case II*

L_s (μm)	η_s	d_s(μm)	d(μm)	$r_{\max}$ (Å.min)	w_1^*	w_2^*
10	0.5	1	1	250	1,000	40

*Cycle time is considered.

Table 4. Results for Case II*

OOW			EOW		
$L(t_f)$ (μm)	$\eta(t_f)$	t_f (min)	$L(t_f)$ (μm)	$\eta(t_f)$	t_f (min)
9.36	0.58	69.14	11.14	0.87	46

*Cycle time is considered.

Table 5. Parameters for Case III*

L_s (μm)	η_s	d_s(μm)	d(μm)	$r_{\max}$ (Å/min)	w_1^*	w_2^*
10	0.5	1	0.9	250	40,000	1,000

*$d < d_s$.

Table 6. Results for Case III*

OOW			EOW		
$L(t_f)$ (μm)	$\eta(t_f)$	t_f (min)	$L(t_f)$ (μm)	$\eta(t_f)$	t_f (min)
9.94	0.47	77.06	11.02	0.87	41.40

*$d < d_s$.

Table 7. Parameters for Case IV*

L_s (μm)	ηs	d_s (μm)	d (μm)	r_{max} (Å/min)	w_1^*	w_2^*
10	0.5	1	1.1	250	20,000	1,000

*$d > d_s$.

Table 8. Results for Case IV

OOW			EOW		
$L(t_f)$ (μm)	$\eta(t_f)$	t_f (min)	$L(t_f)$ (μm)	$\eta(t_f)$	t_f (min)
10.00	0.53	82.57	11.25	0.87	50.60

*$d > d_s$.

tional policy should still be used for the situation when the cycle time is critical and wall curvature is not a concern.

Conclusions

The optimal open width design principle is shown to be capable of controlling both the bottom linewidth and the side-wall curvature. An optimal control solution provides the flexibility of achieving a trade-off among the linewidth, the wall curvature, and the cycle time. Operators can thus adjust the process to accomodate various requirements such as product specifications and delivery time. However, if the wall curvature is not a concern, EOW is a better choice than OOW, since the cycle time is significantly lower. This study explores how to introduce the new idea of optimal open width design into thin-film manufacturing processes.

Acknowledgment

This research is funded by the Storage Technology Corporation. The authors gratefully acknowledge the support and help provided by Dr. Subrata Dey, Mr. Barry McPherron and Dr. Richard Talcott.

Notation

J = performance index
J^* = dimensionless performance index
$L(t)$ = bottom linewidth at any time after breakthrough, μm
$L(t_f)$ = final value of bottom linewidth, μm
$L^*(t_f^*)$ = dimensionless final value of bottom linewidth
R_s = scaling factor for undercut, μm
$R(t)$ = undercut at any time after breakthrough, μm

Greek letters

$\eta(t)$ = side-wall curvature at any time after breakthrough, dimensionless
$\eta(t_f)$ = final value of side-wall curvature, dimensionless
$\eta^*(t_f^*)$ = scaled final value of side-wall curvature, dimensionless

Literature Cited

Barouch, E., and B. D. Bradie, "Resist Development Described by Least Action Principle—Line Profile Prediction," *J. Vac. Sci. Technol. B*, **6**(6), 2234 (1988).

Boehm, H., "Adaptive Control to a Dry Etch Process by Microcomputer," *Automatica*, **18**(6), 665 (1982).

Carrier, G. F., and C. E. Pearson, *Partial Differential Equations—Theory and Technique*, Academic Press, New York, p. 271 (1976).

Carroll, T. A., "On-Line Indentification and Optimal Control of the Positive Optical Microlithrographic Spray Development Process Using Interferometry," PhD Thesis, Univ. of Colorado, Boulder (1990).

Carroll, T. A., and W. F. Ramirez, "On-Line State and Parameter Identification of Positive Photoresist Development," *AIChE J.*, **36**(7), 1046 (1990).

Carroll, T. A., and W. F. Ramirez, "Development of Positive Optical Photoresists: Adaptive Control," *Chem. Eng. Sci.*, **48**(12), 2239 (1993).

Crisalle, D. D., R. A. Soper, D. A. Mellichamp, and D. E. Seborg, "Adaptive Control of Photolithography," *AIChE J.*, **38**(1), 1 (1992).

Kern, W., and C. A. Deckert, "Chemical Etching," *Thin Film Processes*, Vol. 1, J. L. Vossen and W. Kern, eds., Academic Press, New York (1978).

Lauchlan, L., K. Sautter, T. Batchelder, and J. Irwin, "In-line Automatic Photoresist Process Control," *SPIE: Adv. Resist Technol. Process. II*, **539**, 227 (1985).

Litchtenberg, A. W., D. M. Lea, and F. L. Lloyd, "Investigation of Etching Techniques for Superconductive Nb/Al-Al_2O_3/Nb Fabrication Processes," *IEEE Trans. Appl. Superconduct.*, **ASC 3**(1), 2191 (1993).

Moreau, W. M., *Semiconductor Lithography Principles, Practices, and Materials*, Plenum Press, New York (1988).

Morgan, J., *Introduction to Geometrical and Physical Optics*, McGraw-Hill, New York (1953).

Oh, S., Y. Choi, Y. Kwon, and C. Kim, "Etched Profiles of SiO_2 Layer," *Electron. Lett.*, **17**(6), 227 (1981).

Pontryagin, L. S., R. V. Boltyanskii, R. V. Gamkrelidze, and E. F. Mischenko, *The Mathematical Theory of Optimal Processes*, Wiley, New York (1962).

Ramirez, W. F., *Process Control and Identification*, Academic Press, San Diego (1994).

Zhou, B., and F. W. Ramirez, "Modeling and Control of Wet Etching," *Proc. IFAC World Congress*, Vol. B, p. 187 (1996a).

Zhou, B., and F. W. Ramirez, "Kinetics and Modeling of Wet Etching of Aluminum Oxide by Warm Phosphoric Acid," *J. Electrochem. Soc.*, **143**(2), 619 (1996b).

Manuscript received Sept. 11, 1995, and revision received Feb. 8, 1996.